Simulation of Occupant Posture Change during Autonomous Emergency Braking and Occupant Kinematics in Frontal Collision.

Katsunori Yamada, Mitsuaki Gotoh, Yuichi Kitagawa, Tsuyoshi Yasuki

Abstract Occupant posture change during autonomous emergency braking (AEB) and occupant kinematics in frontal collision were simulated using finite element (FE) models. The human body FE model, THUMS, was used to represent the occupant. Muscle elements were activated for simulating reactions of the occupant retaining the initial posture. Small female, mid-size male and large male occupants were assumed. A forward deceleration of 9.8 m/s^2 was applied to simulate braking by AEB. The emergency locking retractor (ELR) was activated before the time of collision with AEB while in collision without AEB. Frontal collision was simulated by applying a collision pulse to the model. The pre-tensioner and the airbag were activated. For each occupant, injury values were compared between cases with and without AEB. It was assumed that the collision speed was reduced by 20 km/h with AEB. The occupant moved forward during braking. Tensile force was generated in the seatbelt prior to the collision. The distance between the occupant and the steering wheel (airbag) at the time of collision was shorter than that without AEB. However, the maximum forward displacement was smaller and the injury values were lower with AEB. Similar trends were commonly observed in the different body size models.

Keywords autonomous emergency braking, frontal collision, human body FE model.

I. INTRODUCTION

The purpose of autonomous emergency braking (AEB) is to avoid collisions or to lower the collision speed by decelerating the vehicle prior to an event. The accident data generally indicates lower injury risk at lower collision speed [1-2]. During braking, the occupant tends to move forward possibly shortening the distance to the instrument panel or steering wheel. A few studies have been conducted to investigate the influence of such posture change on occupant kinematics in frontal collision. One approach is to measure the posture change of volunteer subjects during braking. An optical motion tracking system is commonly used to capture occupant kinematics in a decelerated vehicle. Muscle activity is also measured with electromyography (EMG) to understand biological responses of actual occupants. Crash test dummies are used to measure injury values in vehicle collision tests. Efforts were made to investigate the influence of occupant posture change on injury values using the 50th percentile Hybrid III dummy [3]. Another approach is to simulate the occupant posture change and impact kinematics using numerical human body models. Muscle elements were introduced for mimicking reactions of volunteer subjects during braking [4-5]. Injury values were compared between cases with and without braking. Multi-body models are useful for simulating occupant motion in a short computational time but have limitations in injury prediction. Finite element (FE) models can precisely describe the human body structure and has the capability of accurate injury prediction. However, FE models usually require a long computational time. The durations of events are quite different between braking and collision. Deceleration during braking can last for a second while the duration of high speed collision is around 0.1 second. Efforts were made to connect braking and collision simulations conducted separately [5]. Care must be taken when connecting two simulations so that forces and stress/strain calculated in the first simulation are transferred to the second simulation. Most of such studies focused on a mid-size male occupant (AM50), while few studies included small and large occupants. This study conducted full scale simulations before and during frontal collision taking into account occupant posture change for different body size occupants. The study objective was

K. Yamada is Assistant Manager of Impact Biomechanics Group, Advanced CAE Division in TOYOTA MOTOR CORPORATION in Toyota, Japan (Ph. +81 565 94 2135, fax. +81 565 94 2060, e-mail: katsunori_yamada@mail.toyota.co.jp). M. Gotoh is Assistant at TOYOTA, Y. Kitagawa, Ph.D., is General Manager at TOYOTA and T. Yasuki, Ph.D., is Project General Manager at TOYOTA.

to simulate occupant posture change during AEB and occupant kinematics in frontal collision and to discuss possible effectiveness of AEB to help lower injury values for different body size occupants.

II. METHODS

Two simulations were performed separately, one for a pre-collision phase with the THUMS Version 5 to predict the posture change of the occupant during braking (AEB), and the second for a collision phase with the THUMS Version 4 to calculate injury values in a frontal collision. The THUMS Version 5 was developed to simulate muscular responses of the occupant in the pre-collision phase while the THUMS Version 4 aimed to simulate injuries in vehicle collisions. A technique was used to perform the pre-collision and collision simulations seamlessly. Figure 1 shows the simulation flow from the pre-collision phase to the collision phase. Before performing the simulations, the occupant model was placed onto the seat model and was stabilised under the gravity. In the pre-collision phase with THUMS Version 5, braking deceleration was applied to the cabin model simulating AEB. The time history curves of displacement and rotation angle of the head, chest and pelvis were output from the model. The trajectory of the occupant during braking was generated by THUMS Version 5. In the collision phase, the THUMS Version 4 occupant model was guided along the trajectory so that the body parts moved along the displacement and rotation angle obtained in the pre-collision phase. The muscle forces of THUMS Version 5 calculated during pre-collision phase were not transferred to THUMS Version 4. The seatbelt tension and the seat reaction force in the pre-collision phase were reproduced in the beginning of the collision phase. Then, a collision pulse was applied to the cabin model to simulate the frontal collision. The simulations were performed for small female, mid-size male and large male occupants. The THUMS Version 5 AM50 was used for representing the mid-size male occupant and was scaled for representing small female and large male occupants. The THUMS Version 4 AF05, AM50 and AM95 were used for representing three body size occupants. The THUMS series has been jointly developed by TOYOTA MOTOR CORPORATION and TOYOTA Central R&D Labs., Inc. in Nagakute, Japan. Activation of neck, chest, abdomen and lower limb muscles was approximated for simulating muscle tone of living human subjects.

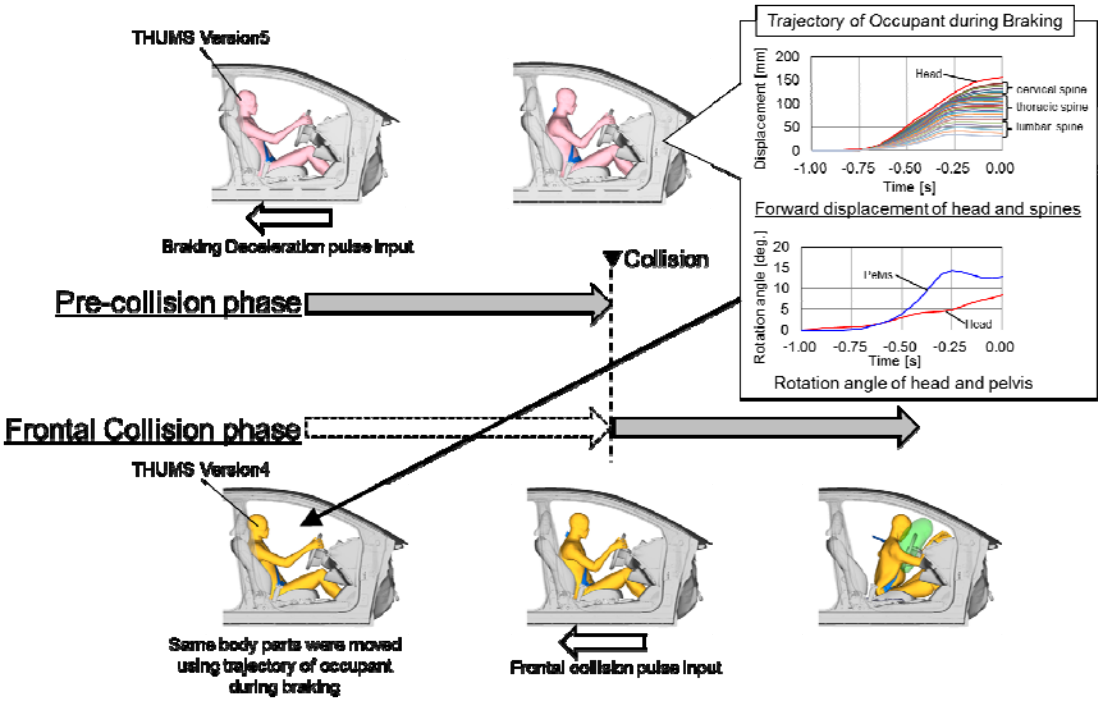

Fig. 1. Simulation Flow from Pre-collision Phase to Frontal Collision Phase.

Occupant Model

As described previously, the THUMS Version 4 and Version 5 were used for representing the small female, mid-size male and large male occupants. The THUMS Version 4 is characterized by its fine mesh for precisely representing the human body structure. The typical mesh size in THUMS Version 4 was around 3-5 mm while that in THUMS Version 5 was 5-10 mm. The THUMS Version 4 AF05 geometry was based on a CT scan data of a small female and was adjusted to the anthropometric dimensions of AF05 with a height of 153 cm and a weight of 46 kg. The THUMS Version 4 AM50 geometry was based on a CT scan data of a mid-size male and was adjusted to the anthropometric dimensions of AM50 with a height of 175 cm and a weight of 77 kg. The THUMS Version 4 AM95 geometry was generated by scaling the AM50 and was adjusted to the anthropometric dimensions of AM95 with a height of 188 cm and a weight of 101 kg. The tissue material properties were defined based on the literature data [6-7]. The mechanical responses of the model against various impacts were validated to the literature data [8-9]. The Version 4 model is capable of simulating injuries frequently caused in vehicle collisions, such as bony fracture, ligament rupture, brain damage, internal organ injury, etc. The THUMS Version 5 AM50 occupant model was updated on the THUMS Version 3 AM50 occupant model introducing muscle elements for simulating bracing of a mid-size male occupant. The muscle-tendon complexes were modeled by Hill-type truss elements and seatbelt (tension-only) elements. The muscular responses of the THUMS Version 5 AM50 occupant model were validated to those reported in the literature [10-11]. For this study purpose, small female (AF05) and large male (AM95) models were generated based on the AM50 model. The model geometries were scaled so that the height values matched those of AF05 and AM95, respectively. The body weight values were adjusted by changing the density values of soft tissue (flesh) parts. As a result, the height and weight values of the AF05 and AM95 models were equal to those of THUMS Version 4 AF05 and AM95, though the width and depth values were not exactly the same. The muscle forces were also scaled based on the ratios of height differences from AM50.

Seat Model

A common configuration of vehicle seats includes a cushion, a seatback and a head restraint. Each part has components such as frames, springs, urethane foams and covers. Connecting parts and adjusting gears are also installed. The cushion frame is mounted on longitudinal rails for sliding back and forth. An FE model of a prototype seat was generated for this study. The prototype seat had the common configuration and components described above. Solid elements were used for representing the urethane foams; shell elements were used for the frames and covers; one-dimensional elements were used for the springs. Elasto-plastic material was assumed for the metal parts; low density foam material was assumed for the urethane foam; fabric material was assumed for the seat cover; and kinematic joints were used for representing the adjusting gears. Such modelling techniques are commonly used for generating production seat models. Figure 2 shows the seat FE model used for the study. The validity of mechanical responses of the seat model was previously examined in a frontal impact sled simulation. Pelvis motion of a Hybrid III model was compared to that of a physical dummy test in the same condition. Good agreement was found between the simulation and the test.

Modeling of Muscles

The THUMS Version 5 has the main skeletal muscles of the whole body except the head and face. Ten (10) muscle groups, as shown in Figure 3, were activated in this study. The selected muscle groups played a main role in a reflex action for retaining the initial sitting posture during unexpected braking deceleration (AEB). The sternocleidomastoid muscle is one of the largest and most superficial cervical muscles, passing obliquely across the lateral side of the neck, originating from the manubrium sterni and the medial portion of the clavicle, inserting into the mastoid part of the temporal bone and the superior nuchal line. The longus capitis muscle originates from the transverse processes of C3-C6, and inserts into the inferior surface of the basilar part of the occipital bone. The splenius capitis muscle arises from the nuchal ligament and the spinous processes of C7-T3, and inserts into the mastoid process of the temporal and occipital bone. The semispinalis capitis muscle originates from the transverse processes of the inferior cervical and superior thoracic columna. The trapezius muscle is one of the large superficial muscles, extending longitudinally from the occipital bone to the lower thoracic vertebrae and laterally to the spine of the scapula. The erector spinae muscle extends vertically

throughout the lumber, thoracic and cervical regions, and lies in the groove to the side of the vertebral column. It is covered in the lumbar and thoracic regions by the thoracolumbar fascia, and in the cervical region by the nuchal ligament. The abdominal oblique muscle is constructed of internal and external oblique muscles. The muscular fibers of internal and external oblique muscle run perpendicularly to each other. The inner abdominal oblique muscle is a muscle in the abdominal wall that lies below the external oblique and just above the transverse abdominal muscles. The external abdominal oblique muscle is the largest and the most superficial of the three flat muscles of the lateral anterior abdomen. The rectus abdominis muscle is a paired muscle running vertically on each side of the anterior wall of the abdomen and extends from the pubic symphysis, pubic crest and pubic tubercle inferiorly, to the xiphoid process and costal cartilages of the 5th to 7th ribs superiorly. The quadratus lumborum muscle originates via aponeurotic fibers into the iliolumbar ligament and the internal lip of the iliac crest. It inserts from the lower border of the last rib for about half its length, and by four small tendons from the apices of the transverse processes of the upper four lumbar vertebrae. The hamstrings muscle is any of the three tendons contracted by three posterior thigh muscles (semitendinosus, semimembranosus and biceps femoris). The hamstring tendons make up the borders of the space behind the knee; the muscles are involved in knee flexion and hip extension. One-dimensional Hill-type elements were used to represent the muscles. Muscle branches were not represented. The antagonists were not activated.

Fig. 2. Prototype Seat FE Model.

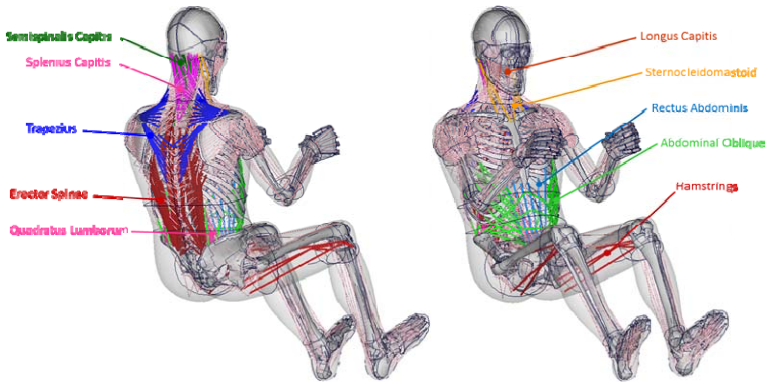

Fig. 3. THUMS Version 5 and Activated Muscle Groups.

Prediction of occupant posture change

The occupant tries to retain the initial sitting posture activating the 10 muscle groups when the occupant moved forward during braking. The study assumed reflex action of the muscles when vehicle was unexpectedly decelerated by AEB. A closed loop control system was adopted to mimic the muscular reaction. Muscle forces were calculated and updated at every time-step of simulation. The displacement, rotation angle, velocity and angular velocity of the occupant head and chest were monitored and fed back to the muscle elements for simulating the reflex action trying to retain the initial sitting posture. Figure 4 shows the image of the closed loop control system adopted in this study.

Muscle activity retaining posture during braking

Muscle forces during braking were identified by simulating autonomous braking tests with twenty (20) volunteers (eleven male and nine female) [12]. The initial speed of the vehicle was approximately 70 km/h, and was decelerated to 20 km/h approximately within two seconds. The maximum braking deceleration was 1.1G. The volunteers did not know the timing of braking in advance. Front passenger kinematics, electromyographic responses, and shoulder belt forces were recorded in the test. The male volunteer data were used for identification of muscle forces to be implemented in the THUMS Version AM50 occupant model. The average height and weight of the male volunteers were 178.2 cm and 77.5 kg, respectively. A cabin model was generated for simulating the volunteer test. The occupant model was placed onto a production seat model. The gravity was applied to the cabin model for a duration of 1.0 second to stabilise the sitting posture on the seat. It

was confirmed that the head position, head angle and T1 position of the occupant model were within the corridor of those of male volunteers. A three-point seatbelt model was fitted around the occupant model. The retractor model was adjusted to the specification as described in their report. Then braking deceleration was applied to the cabin model. Figure 5 shows the average deceleration time history curve measured in the male volunteer tests. A proportional-differential (PD) controller was used for the identification of muscle forces. The PD controller adjusted the muscle activity so that the displacement (proportional) and velocity (differential) of the head and the chest traced the average male volunteer data. The identification was achieved for all muscle groups at every time-step of simulation. For example, the muscle activity of erector spinae was adjusted so that the difference in T1 forward displacement and velocity of the occupant model and the average male volunteer data was minimized. Figure 6 shows the forward and upward displacements of the head centre of gravity (COG) and T1, the head rotation and the shoulder belt force. The male volunteer data are shown as corridors while the calculated data are shown as curves. The displacement and rotation angle of the occupant model were found within the test corridor. The study assumed that the muscle force in reflex action was proportional to the amount of head-T1 motion. The muscle activity was described as functions of the displacement (rotation angle) and the velocity (angular velocity) of the head and the chest using statistics technique, and was incorporated in the closed loop control system. The same function was used for both the AF05 and AM95 models, but the force magnitude was scaled for each body size as there was no test data available for the target size. The scaling ratios for the AF05 and AM95 models were 0.764 and 1.154, respectively, corresponding to the ratios of muscle volumes. Table I shows the relation between the occupant motion and controller (muscle group).

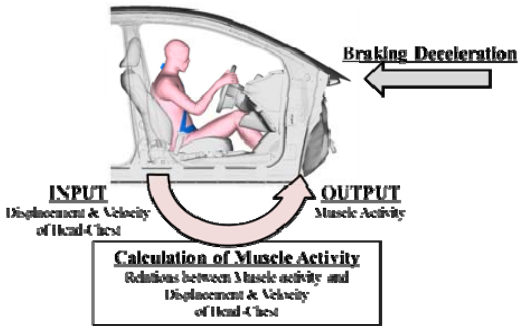

Fig. 4. Closed Loop Control System for Muscle Activity.

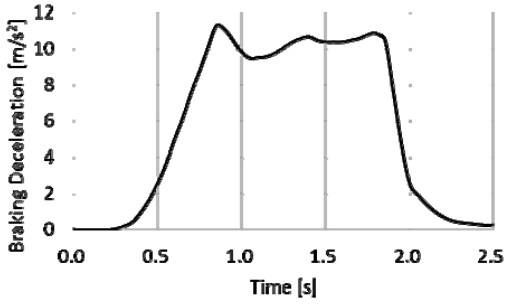

Fig. 5. Braking Deceleration Pulse.

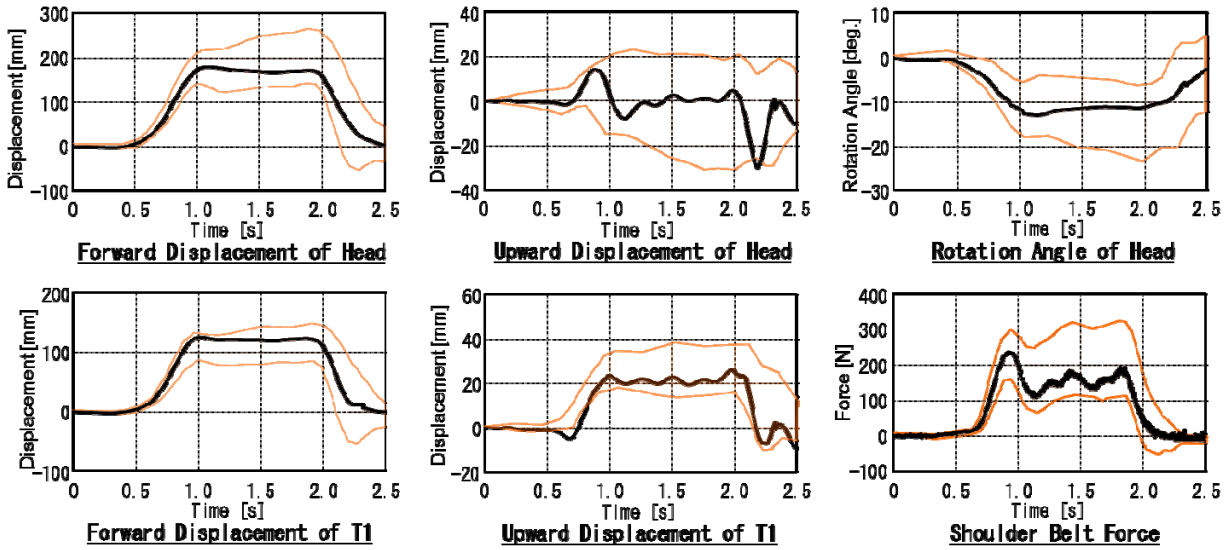

Fig. 6. Forward and Upward Displacement of Head and T1, Rotation Angle of Head, Shoulder Belt Force.

TABLE I

RELATION BETWEEN OCCUPANT MOTION AND CONTROLLER (MUSCLE GROUP)

Occupant Motion	Controller (Muscle group)
Head Forward Motion	Sternocleidomastoid Splenius Capitis
Head Pitching (Rotation) Motion	Longus Capitis Semispinalis Capitis
T1 Forward Motion	Rectus Abdominis Erector Spinae
T1 Upward Motion	Hamstrings
Head Lateral Motion	Trapezius
T1 Lateral Motion	Abdominal Oblique Quadratus Lumborum

Braking and Frontal Collision Simulation

The occupant kinematics were compared with and without AEB. For each of the three different sized occupants, the following collision cases were assumed. The first one was a frontal collision at a speed of 56 km/h without AEB (corresponding to FMVSS208 full overlap frontal impact test to rigid wall). The second one was a frontal collision at a speed of 36 km/h decelerated from 56 km/h by AEB. For comparison purposes, an additional case was conducted assuming a frontal collision at a speed of 56 km/h with AEB with the AM50 occupant. Figure 7 shows the cabin models with the AF05, AM50 and AM95 occupants. The AM50 and AF05 model were placed onto the seat models following the FMVSS208 protocol. The AM95 model was placed 50 mm rearward compared to the AM50 sitting position [13]. The bottom parts of the seat slide rails were fixed to the cabin. A three-point seatbelt model and a driver airbag model were implemented in each model. The seatbelt was fitted around the occupant body. The seatbelt model had a retractor element with a function of ELR, pre-tensioner and load-limiter. The ELR was activated when the cabin deceleration reached 0.45 G. The seatbelt pre-tensioner and the airbag were activated at 11 ms after the initiation of collision. The load-limiter value was set to 4 kN. In the case with AEB, the simulation was performed by two steps as described in Figure 1. In the pre-collision phase, the braking deceleration was applied to the cabin model. The ELR was activated before the frontal collision. In the collision phase, a fontal impact pulse was applied to the cabin model. Figure 8 shows the time history curve of the impact pulse. In this study, the time of collision was defined as 0 ms. In the case without AEB, ELR was activated after the initiation of collision. The durations of the pre-collision phase and the collision phase were 1.0 s and 120 ms, respectively. Table II shows the simulation matrix, including seven (7) cases in total. Case 1 and Case 2 compared the AF05 occupant kinematics without and with AEB. Case 3 and Case 4 compared the AM50 occupant kinematics without and with AEB. Comparison of Case 3 and Case 5 shows the difference in the AM50 occupant kinematics without and with AEB under the same collision speed. The purpose was to isolate the influence of posture change by AEB on the injury values. Case 6 and Case 7 compared the AM95 occupant kinematics without and with AEB. The calculated injury values were; HIC15 for the head; Fz (tension and compression) and Nij for the neck; G 3 ms clip and mid sternum deflection for the chest. Head G

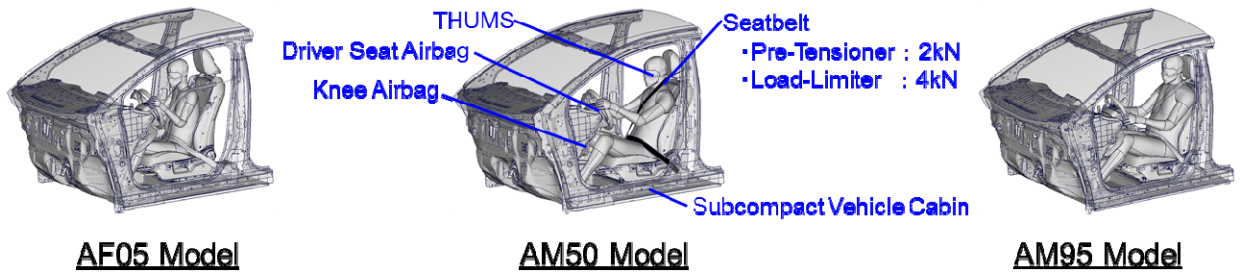

Fig. 7. Cabin and Occupant Models.

was measured at a node represented the center of gravity of the head, constrained rigidly with the skull. Neck force was measured at a cross section fixed between C2 and C3, corresponding to the upper neck load cell of HIII dummy. Chest G was measured at T12. The study did not discuss the absolute injury values but compared

the ratios of the calculated injury values against the reference values (IAV/IARV).

TABLE II
SIMULATION MATRIX

Case	Occupant	Sitting Position (w.r.t. AM50)	Initial Speed [km/h]	Collision Speed [km/h]	AEB Activation	ELR Activation Time
1	AF05	160mm Forward	56	56	No	11 ms
2	AF05	160mm Forward	56	36	Yes	Before Collision
3	AM50	-	56	56	No	11 ms
4	AM50	-	56	36	Yes	Before Collision
5	AM50	-	76	56	Yes	Before Collision
6	AM95	50mm Rearward	56	56	No	11 ms
7	AM95	50mm Rearward	56	36	Yes	Before Collision

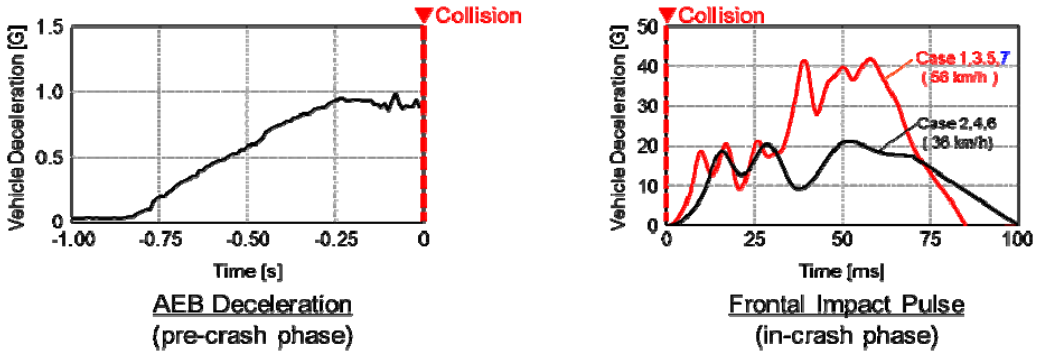

Fig. 8. Braking Deceleration (AEB) and Frontal Impact Pulse.

Ride-Down Effect

Kinematic energy of the occupant at the timing of frontal collision E_0 is absorbed by both the vehicle and the restraint system. The energy absorbed by the vehicle is defined as ride-down energy E_{rd} while the energy absorbed by the restraint system is defined as restraint energy E_{rs}. The relationship of the energy componets can be expressed as follows:

$$E_0 = \int F\,dx_0 = \int F\,dx_v + \int F\,dx_{ov} = E_{rd} + E_{rs}$$

Where F is contact force between the occupant and the restraint system, x_0 is the occupant forward displacement in the global coordinate system, x_v is the vehicle forward displacement in the global coordinate system, and x_{ov} is the occupant forward displacement in the vehicle coordinate system. The ride-down effect is calculated as the ratio of ride-down energy E_{rd} to the occupant kinematic energy E_0 as follows:

$$Ride-Down\ Effect = \frac{E_{rd}}{E_0}$$

III. RESULTS

The study assumed that the validated THUMS could simulate the occupant kinematics in the pre-collision phase and in the frontal collision phase, and show comparable responses in the cases with and without AEB.

Occupant Posture in Pre-collision Phase

Figure 9 compares the occupant postures in the lateral view at the time of collision for all cases. The occupants in Case 1, Case 3 and Case 6 show their initial sitting postures while the occupant postures in Case 2, Case 4 and Case 7 were obtained from the pre-collision simulations with AEB. The distance between the occupant chest and the steering wheel at the time of collision was shorter than that in the case without AEB in each body size occupant, and was shortest in the AF05 occupant. The distances values with AEB were 55 mm in the AF05, 180 mm in the AM95 and 200 mm in the AM50, while those without AEB were 100 mm in the AF05, 230 mm in the AM95 and 260 mm in the AM50. The occupant posture in Case 5 was exactly the same as that in Case 4. Figure 10 shows the chest forward displacement in the pre-collision phase while Figure 11 shows the contact force between the occupant and the (shoulder and lap) seatbelt. In the case with AEB, the seatbelt was pulled out from the retractor as the occupant moved forward. The ELR was activated at -0.6 seconds when the deceleration reached 0.45 G. The seatbelt was tensed after that and finally balanced the inertial force of the occupant. Then the occupant forward motion stopped at -0.25 seconds. The magnitude of contact force at the time of collision ranged from 150 to 400 N.

Occupant	AF05	AM50		AM95
Without AEB	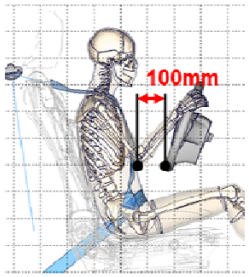 Case 1	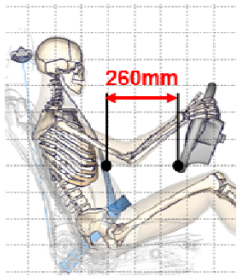 Case 3		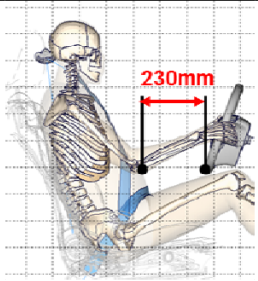 Case 6
	Initial Vel. 56 km/h / Collision Vel. 56 km/h	Initial Vel. 56 km/h / Collision Vel. 56 km/h		Initial Vel. 56 km/h / Collision Vel. 56 km/h
With AEB	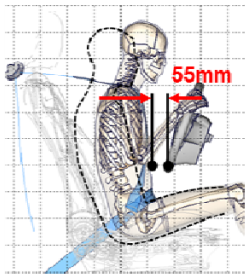 Case 2	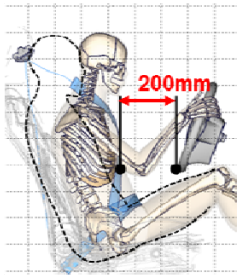 Case 4	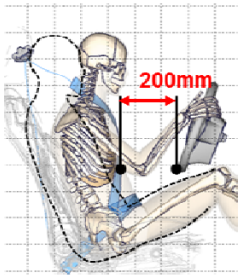 Case 5	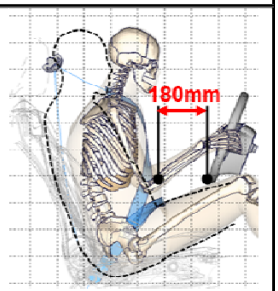 Case 7
	Initial Vel. 56 km/h / Collision Vel. 36 km/h	Initial Vel. 56 km/h / Collision Vel. 36 km/h	Initial Vel. 76 km/h / Collision Vel. 56 km/h	Initial Vel. 56 km/h / Collision Vel. 36 km/h
Seat Position (Comparison with AM50)	160 mm Forward	-		50 mm Rearward

Fig. 9. Occupant Posture at Time of Collision.

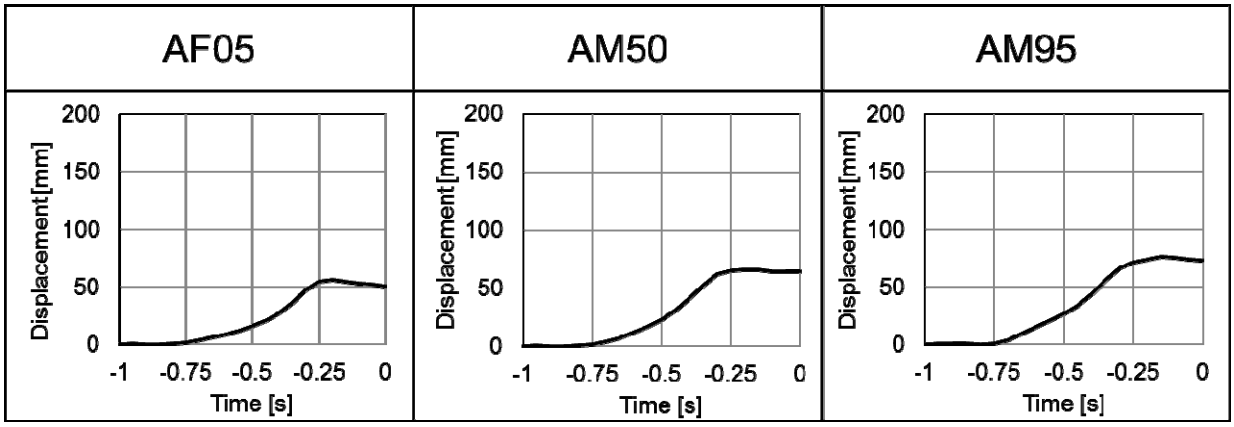

Fig. 10. Chest Forward Displacement (Pre-collision phase in the case with AEB)

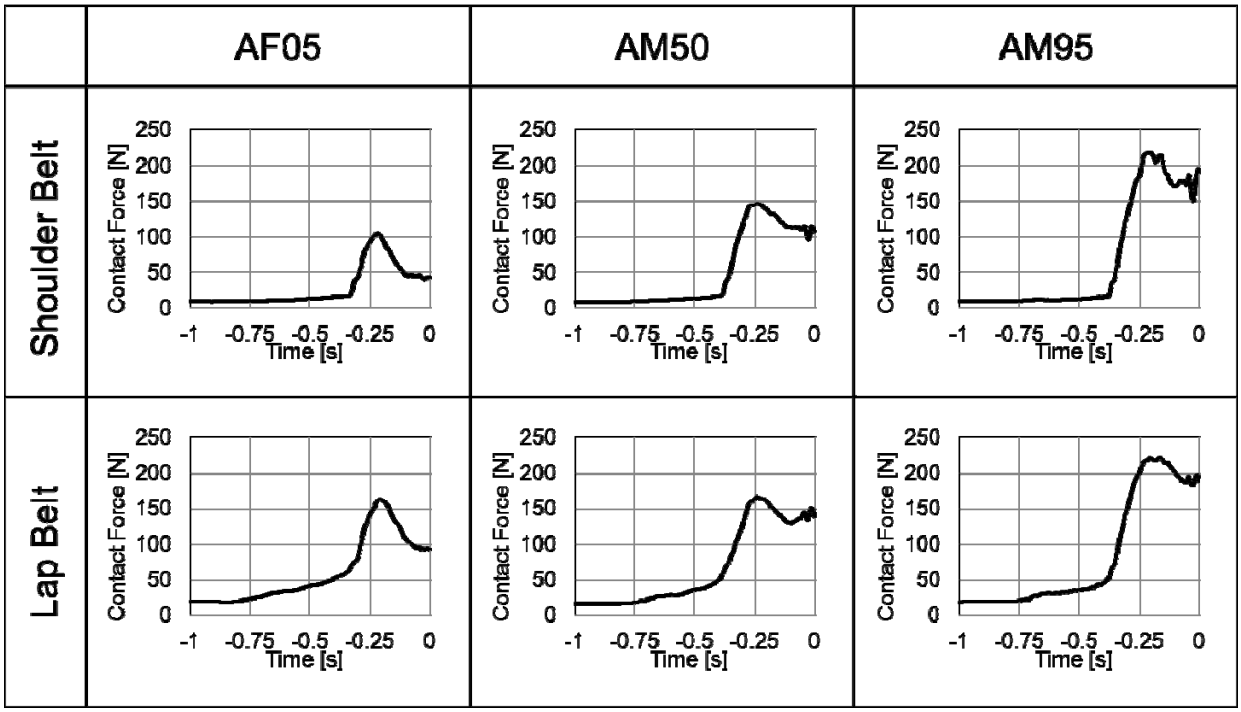

Fig. 11. Contact Force between Occupant and Seatbelt (Pre-collision phase in the case with AEB)

Occupant Posture in Frontal Collision Phase

Figure 12 compares the occupant postures in the lateral view at the time of maximum forward displacement of the head in the frontal collision for all cases. The red lines in the figure were the forward displacements of the head COG and the chest (T12) in the collision phase. In the case with AEB, the maximum forward displacements of the head and chest were smaller than those without AEB despite the occupant came close to the steering wheel during braking. Similar trends were commonly observed in the AF05 and AM95 occupant models.

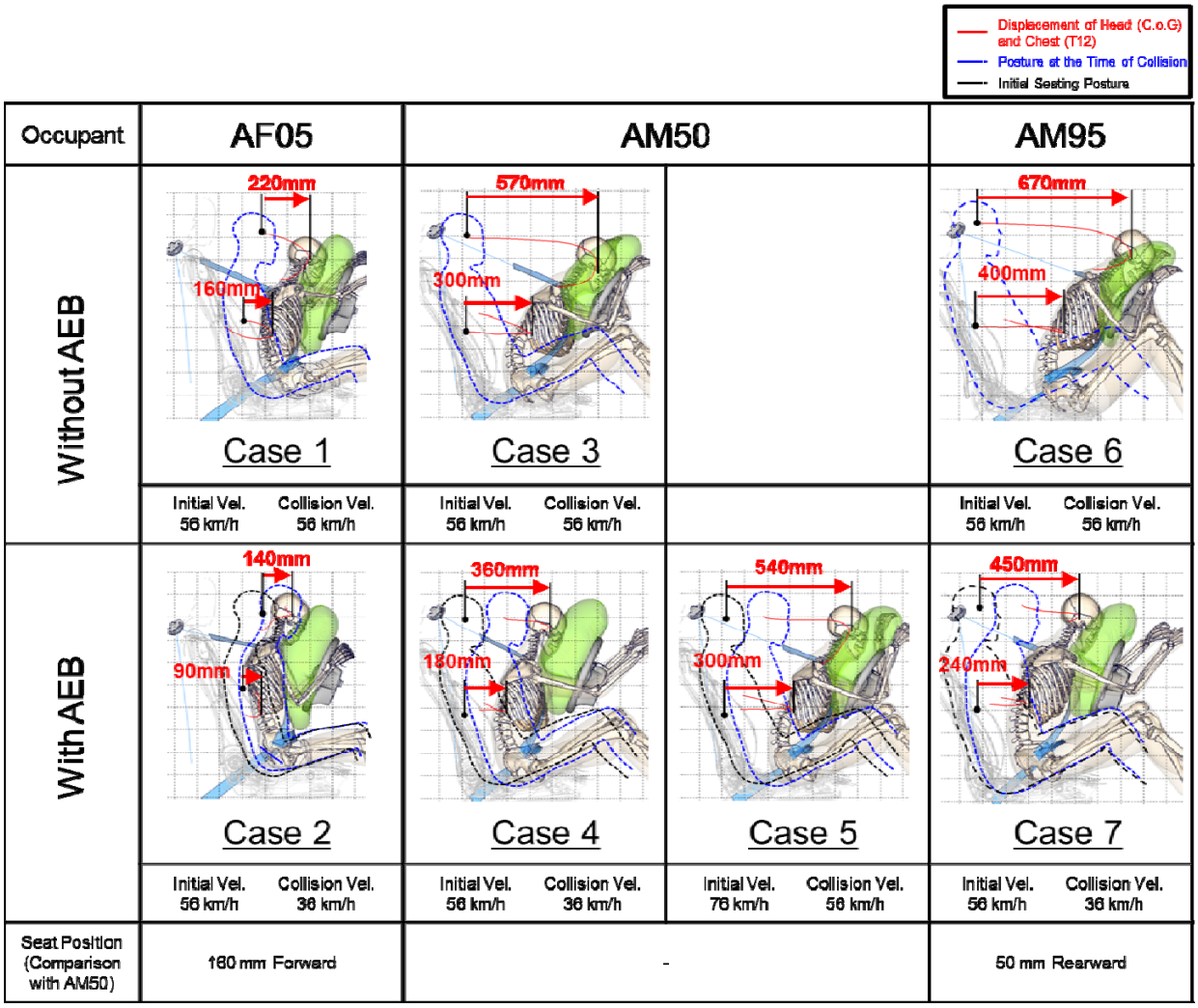

Fig. 12. Occupant Posture at Time of Maximum Head Displacement.

Contact Force between Occupant and Restraint system (seatbelt and airbag)

Figure 13 shows the contact force between the occupant and the seatbelt. The contact force was divided into the shoulder belt and the lap belt. For each occupant, the maximum contact force in the case with AEB was lower than that in the case without. Figure 14 shows the contact force between the occupant and the airbag. The contact force was divided into the head and the chest. In the cases with AEB for the AM50 and AM95 occupants, the contact timing with the airbag was earlier and the maximum contact force was less than in the case without. For the AF05 occupant, no significant difference was noted in the contact timing or in the maximum contact force with and without AEB.

Injury Values

Figure 15 shows injury values for all cases. A common trend was that the injury values of the head and the chest in the case with AEB were lower than those without. The neck injury values in the case with AEB were the same or lower than that without. Figure 16 compares the ride-down effect among all cases. For each occupant, the ride-down effect in the case with AEB was higher than that without.

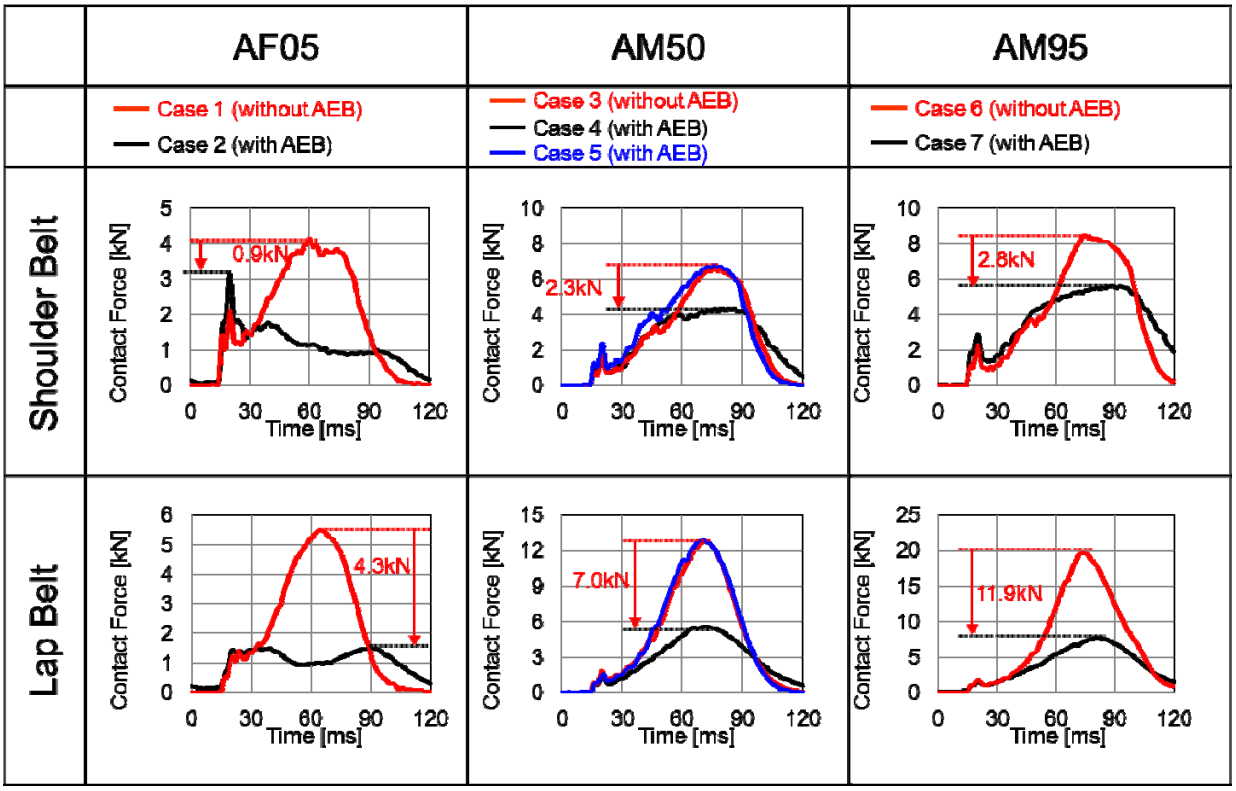

Fig. 13. Contact Force between Occupant and Seatbelt (Frontal collision phase)

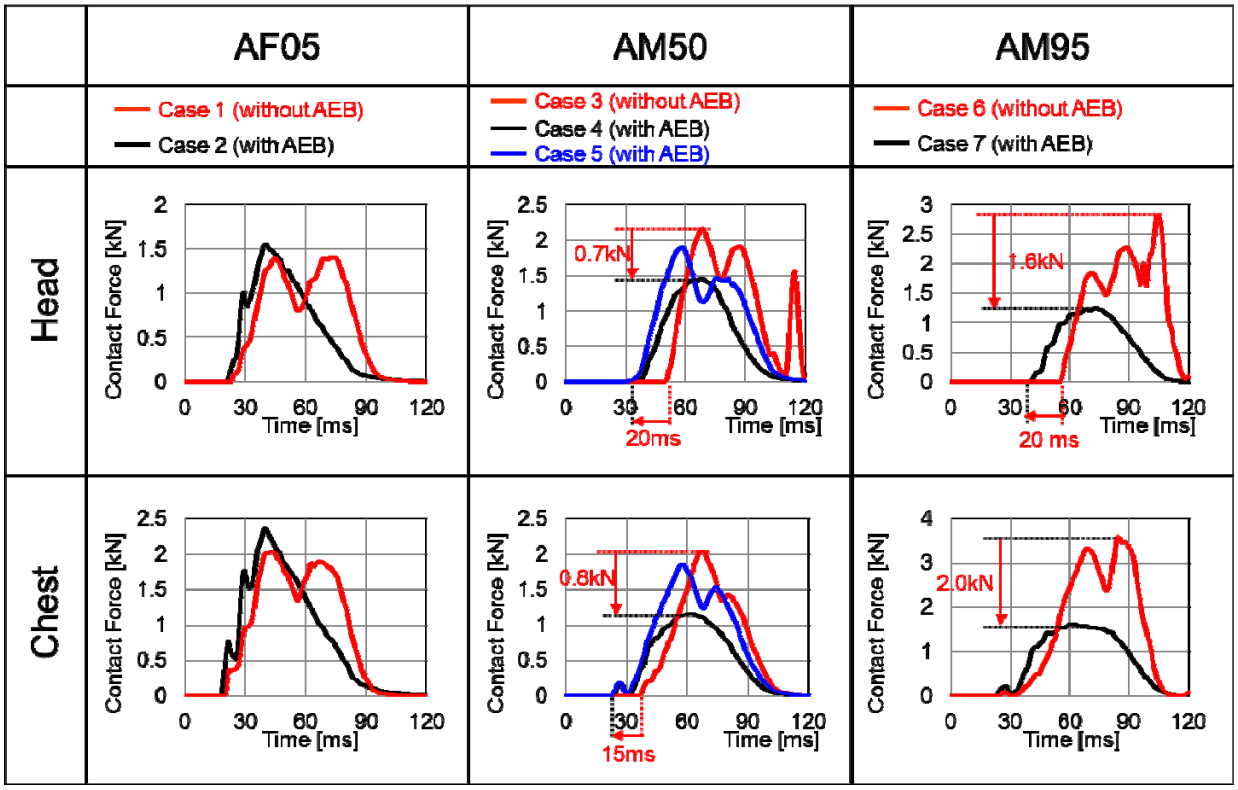

Fig. 14. Contact Force between Occupant and Airbag.

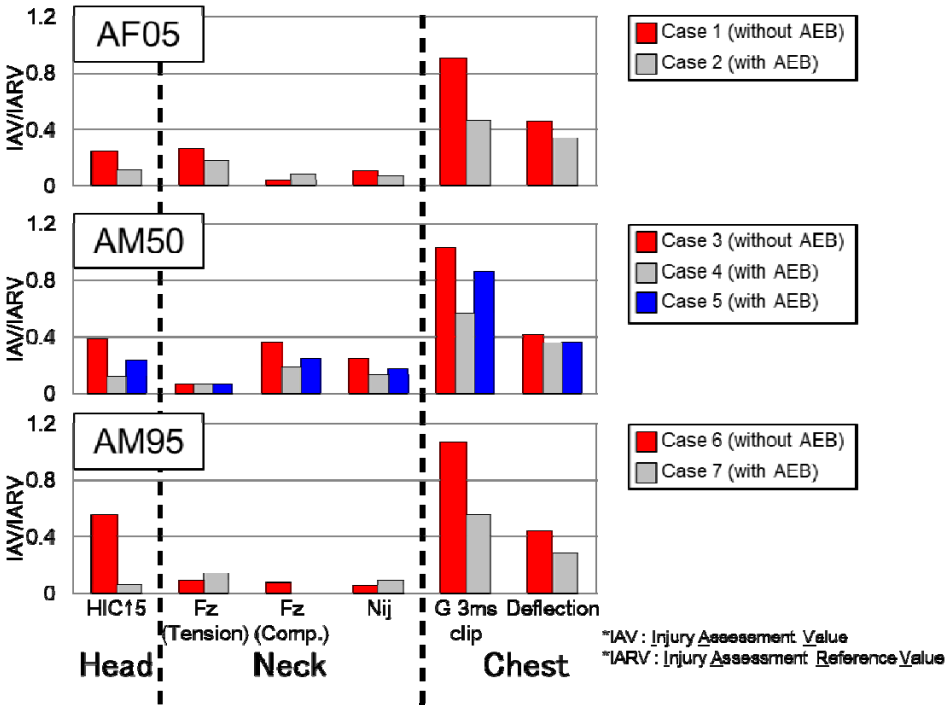

Fig. 15. Injury Values.

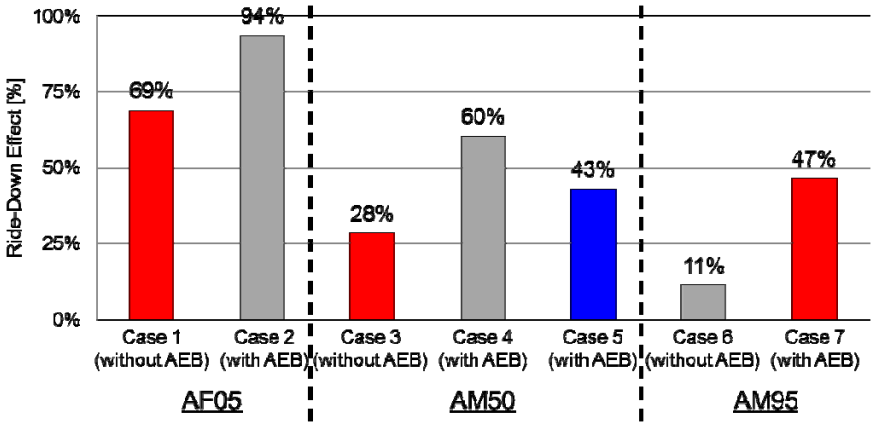

Fig. 16. Ride-Down Effect.

IV. Discussion

Comparison between Case 3 and Case 5 indicates the ride-down effect. The injury values in Case 5 were lower than those in Case 3 despite the same collision speed (Figure 15). The difference between the two cases was the occupant posture and the seatbelt tension at the time of collision. The distance between the occupant chest and the steering wheel in Case 5 was shorter than that in Case 3 (Figure 9). The contact timing between the occupant and the airbag was earlier in Case 5 (Figure 14). Both the tensed seatbelt and the early airbag contact raised the ride-down effect in Case 5 (Figure 16). Comparison between Case 4 and Case 5 indicates the effect of collision speed. The injury values in Case 4 were lower than those in Case 5. This is owing to the lower collision speed and the higher ride-down effect (Figure 16). These results suggest that AEB helps lower the injury values not only by reducing the collision speed but also by raising the ride-down effect. Similar trends were found for the other body size models. However, the ratios of ride-down effect were different among the occupant models. The ride-down effect increased by 25 % in the AF05 (from 69 % in Case 1 to 94 % in Case 2),

while 32 % in the AM50 (from 28 % in Case 3 to 60 % in Case 4), and 36 % in the AM95 (from 11 % in Case 6 to 47 % in Case 7). The distance between the occupant chest and the steering wheel changes with the seating position. The AF05 occupant was close to the steering in the initial sitting position. There was little difference in contact timing with the airbag between the cases with and without AEB (Figure 14). As for the AM95 and AM50, the airbag contact timing was earlier when AEB was activated. That increased the ratio of ride-down effect for those occupants. It should be noted that the occupant forward motion stopped at -0.25 seconds and the posture did not change up to the time of collision. There was no significant difference in head contact speed to the airbag with and without AEB.

V. LIMITATIOMS

The effectiveness of AEB was estimated under the particular braking and collision conditions assumed in this study. The sitting posture and the posture change during braking may vary in actual riding situations. The muscular force could change in every braking event, even in the same driver. The study assumed that the muscular forces for the AF05 and AM95 could be scaled from those for the AM50. Further study is necessary to discuss the effectiveness of AEB in various situations. The results obtained in this research were based on three body sizes, each at a single sitting position. The results suggest that sitting position affects the ride-down effect. Further research should investigate the relative contributions of body size and sitting position. The occupant kinematics during braking were tuned to lie within a single corridor with variation among the volunteer subjects. Muscle responses for the AF05 and AM95 models were not individually tuned but scaled from that of the AM50. More work is needed to examine if the study findings are sensitive to the variation range of volunteer kinematics observed in the AEB tests. The occupant models assumed normal sitting postures. More research is needed to determine if the response could change with and without awareness. The study used a single vehicle geometry, single braking deceleration curve and a single collision pulse. More work is needed to examine the influence of such factors including the impact direction. Interaction among the occupant, seat and seatbelt in the pre-collision phase calculated by THUMS Version 5 was reproduced when the THUMS Version 4 was guided along the trajectory. The interaction was mostly given by the relative position among them. It was assumed that the stress/strain generated on the THUMS Version 4 at the time of collision was realistic. A possible difference was internal force such as generated in the bones due to muscle response. It was assumed that the muscle force in the collision phase was negligible since the magnitude was around 1/10 of the interaction force typically calculated in the collision phase.

VI. CONCLUSIONS

The study simulated the occupant posture change during braking (AEB) and estimated injury values in frontal collision for the AM50, AF05 and AM95 occupants. When AEB was activated, the occupant body moved forward and the maximum forward displacement in the frontal collision was smaller compared to the case without AEB. The injury values were lower than those without AEB. The ride-down effect was raised owing to the tensed seatbelt and the early airbag contact. Similar trends were observed in all three occupant models. The results suggest that AEB helps lower the injury values not only by reducing the collision speed but also by raising the ride-down effect.

VII. REFERENCES

[1] Gabauer D J, Gabler H C, COMPARISON OF DELTA-V AND OCCUPANT IMPACT VELOCITY CRASH SEVERITY METRICS USING EVENT DATA RECORDERS. *ANNU PROC ASSOC ADV AUTOMOT MED, 2006, 50:57-71*.

[2] Rechards D C, Relationship between Speed and Risk of Fatal Injury: Pedestrians and Car Occupants. *Department of Transport*, 2010, London (UK).

[3] Schoneburg R, Baumann K-H, Fehring M, The Efficiency of PRE-SAFE Systems in Pre-braked Frontal Collision Situations. *The 22nd ESV Conference Proceedings*, 2011, Washington, D.C (USA).

[4] Meijer R, Elrofai H, Broos J, Hassel E, EVALUATION OF AN ACTIVE MULTI-BODY HUMAN MODEL FOR BRAKING AND FRONTAL CRASH EVENTS. *The 23nd ESV Conference Proceedings*, 2013, Seoul (Republic of Korea).

[5] Ghosh P, Andersson M, Vazquez M M, Svensson M, Mayer C, Wismans J, A proposal for integrating pre-crash vehicle dynamics into occupant injury protection evaluation of small electric vehicles. *Proceedings of IRCOBI Conference*, 2015, Lyon (France).

[6] Yamada H, Strength of Biological Materials. F.G. Evean, Ed., *The Williams & Wilkins Company,* Baltimore, 1970.

[7] Abe H, Hayashi K, Sato M, Data Book on Mechanical Properties of Living Cells, Tissues and Organs. *Springer-Verlag*, Tokyo, 1996.

[8] Shigeta K, Kitagawa Y, Yasuki T, Development of next generation human FE model capable of organ injury prediction. Procedings of the 21st International Technical Conference on the Enhanced Safety of Vehicles. Stuttgart, Germany, June 15th–18th, 09-0111, 2009.

[9] Watanabe R, Katsuhara T, Miyazaki H, Kitagawa Y, Yasuki T, Research of the relationship of pedestrian injury to collision speed, car-type, inpact location and pedestrian sizes using human FE model (THUMS Version 4). Stapp Car Crash Journal, 2012, 56:269-321.

[10] Iwamoto M, Nakahira Y, Kimpara H, Development and Validation of the Total HUman Model for Safety (THUMS) Toward Further Understanding of Occupant Injury Mechanisms in Precrash and During Crash. *Traffic Injury Prevention*, 2015, 16:1-13.

[11] Iwamoto M, Nakahira Y, Development and Validation of the Total HUman Model for Safety (THUMS) Version 5 Containing Multiple 1D Muscles for Estimating Occupant Motions with Muscle Activation During Side Impacts. *Stapp Car Crash Journal*, 2015, 59:53-90.

[12] Ólafsdóttir J M, Östh J, Davidsson J, Brolin K, Passenger Kinematics and Muscle Responses in Autonomous Braking Events with Standard and Reversible Pre-tensioned Restraints. *Proceedings of IRCOBI Conference*, 2013, Gothenburg (Sweden).

[13] Reed M P, Manary M A, Flannagan C A C, Schneider L W, Arbelaez R A, Improved ATD positioning procedures. SAE Technical Paper Series 2001-01-0117, 2001.